CrossMark

Ferroelectric phase-transition-assisted anomaly in the electric resistivity (FPTAA) of lead-free PTC thermistors

Igor Zajc[1] · Miha Drofenik[1,2]

Abstract

Ceramic composites in the $BaTiO_3$–$(Bi_{1/2}Na_{1/2})TiO_3$ system exhibiting a positive temperature coefficient of electrical resistivity effect were prepared using a conventional solid-state reaction method. The composite samples were sintered in nitrogen to achieve their final-phase properties, a high resistivity jump of ~ 10^3 at about 170 °C. The resistivity anomaly of the composite composed of a conducting network based on a conducting $BaTiO_3$ and a highly resistive ferroelectric phase with a Curie temperature (T_C) of 170 °C was explained in the light of ferroelectric phase-transition-assisted anomaly in the resistivity (FPTAA).

1 Introduction

Donor-doped barium titanate (BT) with a positive temperature coefficient of resistivity (PTCR) is the most investigated thermistor material in recent decades and has found many applications in electronic and electrical engineering. In recent times lead-free PTCR ceramics have been thoroughly investigated in an attempt to replace lead-containing PTCR ceramics because of the hazardous influence of the toxic lead oxide. From the viewpoint of environmental protection, lead-free materials are necessary to replace the classic high-temperature PTCR thermistors that contain lead oxide. Recently, the $BaTiO_3$–$(Bi_{1/2}Na_{1/2})TiO_3$ (BT–BNT) ceramic has appeared as a new, lead-free, PTCR thermistor material with an anomaly in its resistivity above 130 °C that is a possible alternative to lead-containing PTCR ceramics. A large PTCR effect at about 170 °C has been established in lanthanum-doped BT–BNT ceramics [1]. In addition, it was reported that superior PTCR properties can be obtained by the addition of 8.8 mol% BNT to a BT–BNT solid-solution sample sintered in a flow of N_2 [2]. Furthermore, it was described how ceramics prepared with 20 mol% BNT additions, sintered in a flow of N_2, showed a resistivity anomaly

at about 190 °C [3, 4]. All these reports, including [5, 6], indicate that the BT–BNT system exhibits an interesting PTCR characteristic with the maximum temperature of resistivity anomaly up to 190 °C, however, the explanation for this effect remains to be clarified.

In this contribution the incorporation of the BT–BNT solid–solution phase into conducting BT ceramics is considered as an effective way of increasing the temperature of the resistivity anomaly for a PTCR thermistor above 130 °C. The aim of this paper is to make it clear that in this case the mechanism of the PTCR effect can be explained in the light of the ferroelectric phase-transition-assisted anomaly in the resistivity (FPTAA).

2 Experimental procedure

Two constituent phases were used to prepare the composite. The first one (A) was a pure barium titanate from the Ferro company (219-9, Ba/Ti = 0.995, surface area 2.3 m^2/g, and 0.06 wt% impurities). The second constitutive phase (B) was a solid solution of [10 mol% $BaTiO_3$ and 90 mol% $(Bi_{1/2}Na_{1/2})TiO_3$] ≡ $(1 - x)$BT–xBNT, x = 0.9. The BNT was prepared using a conventional ceramic fabrication technique. Powders of TiO_2 and Na_2CO_3 with 99.99% purity and Bi_2O_3 with 99.999% purity were used as the starting raw materials. These oxides and/or carbonate powders were mixed/milled followed by drying and calcining at 800 °C for 2 h. The product was then milled in ethanol for 5 h and dried. The B phase was prepared using a conventional ceramic-fabrication

✉ Igor Zajc
igor.zajc@ijs.si

1 Department for Materials Synthesis, Jožef Stefan Institute, 1000 Ljubljana, Slovenia

2 Faculty of Chemistry and Chemical Engineering, University of Maribor, 2000 Maribor, Slovenia

technique using appropriate amounts of BT and BNT. After mixing in ethanol for 2 h and drying, the mixture was calcined at 1050 °C and then milled in ethanol for 5 h and dried. From the powders A and B a series of samples C with various mixtures from 10 wt% (C1), 20 wt% (C2) to 30 wt% (C3) of B were prepared. The mixtures were homogenized in a ball mill with ethanol for 1 h, dried and pressed at 0.3 MPa into pellets with a diameter of 6 mm and a height of 2 mm. In addition a solid solution $(1-x)$BT–xBNT with the composition $x = 0.14 \equiv$ B′ was synthesized under identical ceramic conditions. The samples were sintered at 1250 °C for 2 h in nitrogen and/or air. The microstructures of the composite samples were inspected using scanning-electron-microscope (model JSM 5800, Jeol, Japan) imaging with back-scattered electrons. The EDX analyses of the constitutive elements were performed in the composite phases using an EDX analyzer (model LINK ISIS 300, Oxford Instruments, UK).

The high-temperature thermodiffraction XRD data in the temperature from 20 °C to 200 °C were obtained by using a powder diffractometer (model X′Pert PRO, PANanalytical, Netherlands) equipped with an Anton PAAR camera operating at 45 kV and 40 mA from room temperature to 1200 °C. In this way, a well-defined powder-diffraction profile was obtained for all the reflections, permitting a detailed analysis of the profile changes associated with the paraelectric-to-ferroelectric phase transition. The cell parameters of B′ were estimated from fitting the XRD patterns. The whole-powder-pattern fitting procedure was employed, where the cell parameters were the fitted parameter using the crystallographic software package Topas™. The contribution of the instrumental broadening of the diffraction lines was described by a convolution of the individual instrumental broadening functions generated from the instrument parameters [7].

The electrical contacts on the sintered samples were made with a Ga/In alloy and the temperature dependencies of the resistance and the capacitance were measured while heating at 3 °C/min in a furnace. The capacitances were measured at 10 kHz with an impedance analyzer (model HP 4192A, Hewlett Packard, USA) and the electrical resistances of the sintered samples were measured with a multimeter (model HP 3457A, Hewlett Packard, USA). In addition, the dilation vs. temperature of the composite sample C2 was measured with a dilatometer (model DIL 402 CD/4, Netzsch, Germany).

3 Results and discussion

The diffraction pattern of C2 shows a tetragonal structure similar to that of the pure BT. All the diffraction peaks of the solid-solutions in C2 samples were indexed according to the published data of the host/basic $BaTiO_3$ (ICCD No. 05-0626), indicating the absence of any by-products (XRD patterns are not shown).

The constituent phases A and B, as well as the composites C1, C2 and C3 sintered in air do not show any anomaly in the temperature dependence of the resistivity, but exhibit a NTC course of resistivity with a high room-temperature resistivity $> 10^9$ Ω cm (curves not shown). When the sintering was performed in a reducing atmosphere of nitrogen the samples C show an anomaly in the resistivity, a PTCR effect, Fig. 1.

When the sintering was performed in a reducing atmosphere of nitrogen the composites with compositions C1, C2 and C3 containing 10, 20 and 30 wt% of B phase, respectively, exhibit a PTCR effect (Fig. 1, curves a, b, c). Of these, the composite C2 has a nearly three-orders-of-magnitude high PTCR effect, see Fig. 1 curve a. Here, it is significant that the PTCR anomaly is, more or less, at the same temperature. On the other hand, the semiconducting constituent $A \equiv BT$ phase shows a typical minor shoulder in the temperature dependence of resistivity at the T_C of BT, see Fig. 1 curve d, whereas the pristine phase B and phase B′ show a high resistivity of $> 10^8$ Ω cm, see Fig. 1 curves e and f, respectively.

Figure 2a shows an SEM image of the polished surface of the composite sample C2 sintered in nitrogen. The image with back-scattered electrons shows that the microstructure consists of two phases: one bright and one dark. The EDX spectrum of the bright phase shows that bismuth is a constituent element of the bright phase, see Fig. 2c. The composition was analyzed with EDX measurements, and 14 mol% of BNT ($x = 0.14$) was determined in the solid solution. In the dark phase the amount of bismuth is small and can be
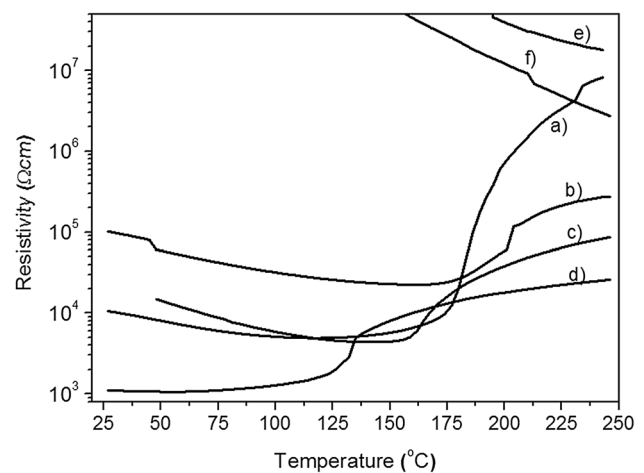
Fig. 1 Temperature dependence of the electrical resistivity of the composite samples and constitutive phases after sintering in nitrogen: curve (*a*) sample C2 (20% B), curve (*b*) sample C3 (30% B), curve (*c*) sample C1 (10% B), curve (*d*) constitutive A phase, curve (*e*) constitutive phase (B) and constitutive phase (B′) curve (*f*)
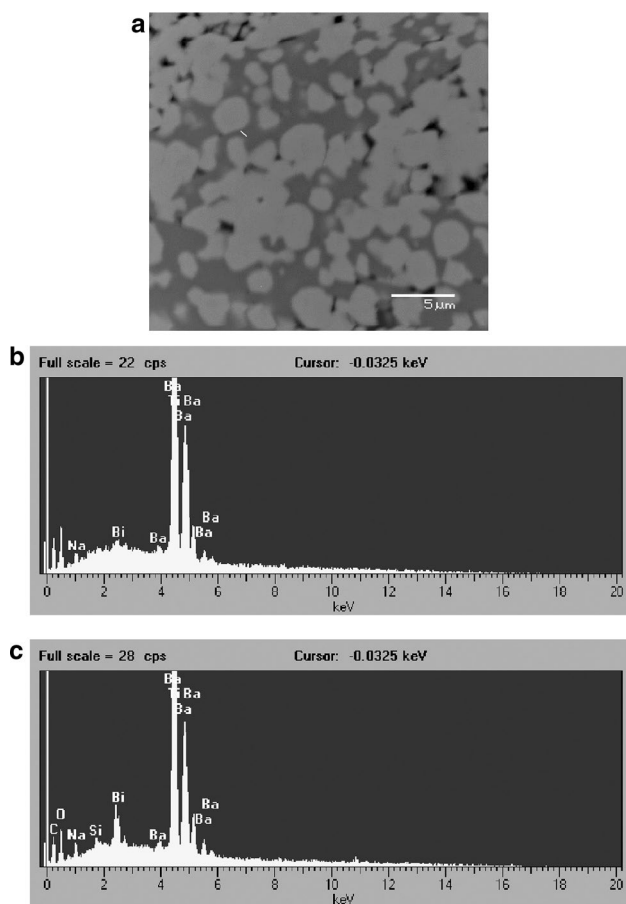
Fig. 2 **a** SEM image with back-scattered electrons of the polished surface of the composite C2 sintered in nitrogen, **b** the EDX spectra of dark phase A and **c** the EDX spectra of Bi-containing bright phase B′

Table 1 Composition of B′ phase in composites C1, C2 and C3

Composite	C1	C2	C3
B′ ≡ $(1-x)$BT–xBNT	$x = 0.13 \pm 0.02$	$x = 0.14 \pm 0.01$	$x = 0.17 \pm 0.03$

Fig. 3 The dielectric constant versus the temperature of the samples sintered in nitrogen: composite C2 curve (*b*) and that of the high-resistivity constitutive phase B curve (*c*)

Fig. 4 DSC spectra of samples sintered in nitrogen: constitutive phase A curve (*a*), composite C2 curve (*b*) and constitutive phase B curve (*c*)

neglected so that it can be anticipated to be the A phase, i.e., BT, see Fig. 2b. Thus, after sintering of the composite C2 in nitrogen the B phase changes its composition to B′, i.e., from $x = 0.9$ to $x = 0.14$. The same phase changes also occur in the other two composites C1 and C3.

As can be seen from the temperature dependence of the resistivity measurements in Fig. 1, the A phase becomes semiconducting BaTiO$_3$ during the sintering in nitrogen (Fig. 1 curve d), while the B and B′ phases retain its high resistance (Fig. 1 curves e and f).

After sintering in nitrogen the B phase in composites C1, C2 and C3 changes its composition to B′ with $x = 0.13$, 0.14 and 0.17 respectively, Table 1, with a Curie
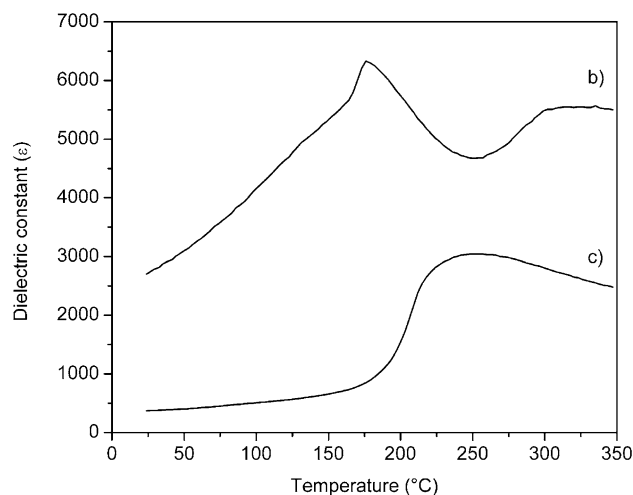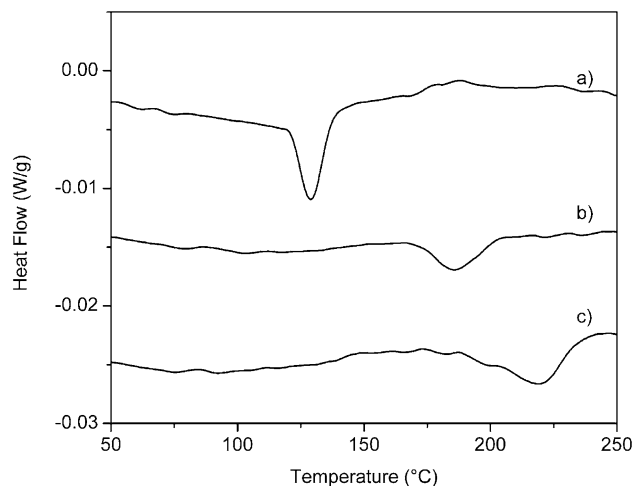
temperature of 170 °C, as shown for the composite C2 in Figs. 3, 4 curves b, i.e., where the dielectric constant versus the temperature is shown, Fig. 3 curve b, and the DSC curve of the composite C2, Fig. 4 curve b. Here, the B′ phase with T_C 170 °C, is the highly resistive phase in the composite C2 (Fig. 1 curve f).

These two phases, A and B′ in the composite C2, govern the course of the temperature dependence of the resistivity of the composite in the measured temperature range. Below the T_C of the composite C2, i.e., the semiconducting BT (A) phase governs the electrical properties of the composite. On the other hand, above the T_C at 170 °C where the disconnection of semiconducting network of

BT occurs the B′ phase determines the main properties of the composite, i.e., a high resistivity.

In brief, while the pure $(Bi_{1/2}Na_{1/2})TiO_3$ exhibits its transition point at about 350 °C [8], its solid-solution (BT–BNT) with 90 mol% BNT, i.e., the pristine B phase, has a T_C at 230 °C, Figs. 3, 4 curve c. The decrease of the Curie temperature of the considered solid solution (BT–BNT) continues after the sintering of the C1, C2 and C3 composites in nitrogen. During the sintering of the composite sample C2 the composition of the solid solution BT–BNT≡ (B) changes to the composition with $x = 0.14$, i.e., to the B′ phase with a Curie temperature of about 170 °C.

Here, we must stress that this composition is fairly close to the ultimate solid solution composition with $x = 0.20$ and $T_C = 175$ °C reported in reference [2] where the Curie points of the solid solutions (BT–BNT) up to the saturation point 20 mol% BNT are given. This Curie temperature is also the highest T_C which the materials in this solid solution system may possess.

Figure 5a shows the thermodiffraction pattern of phase B′ from room temperature up to 200 °C. The splitting of the X-ray diffraction peaks is well defined in terms of symmetry, allowing an analysis of the systematic changes for different (hkl) indices. In our study, the evolution of phase B′ was determined by pattern matching to the laboratory X-ray
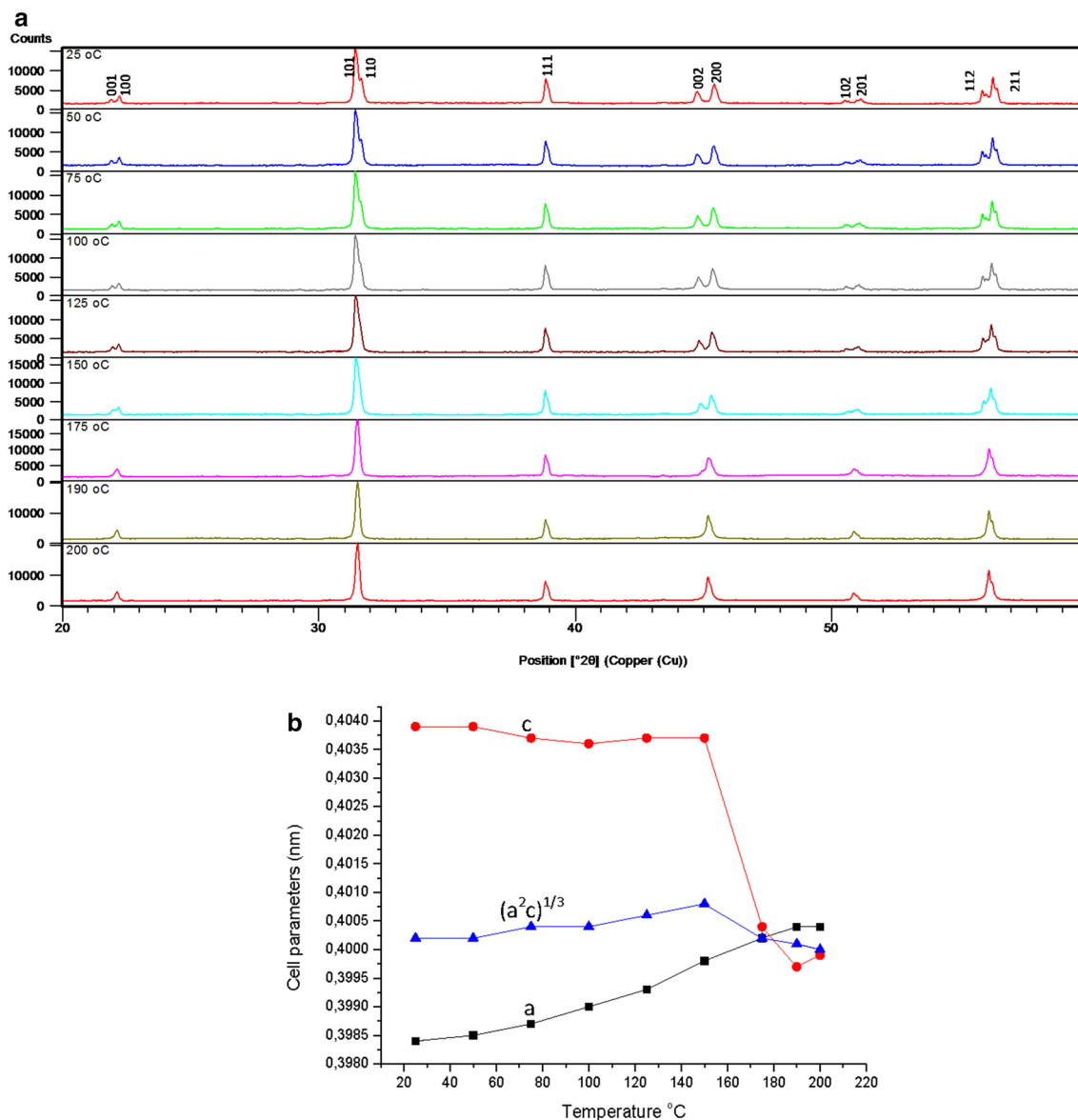

Fig. 5 (a) Thermodiffraction spectra of B′ phase measured at various temperatures from 20 to 200 °C and (b) corresponding cell parameters (a) and (c) and the pseudocubic cell parameter $\sqrt[3]{a^2c}$ (the cube root of the unit cell-volume) versus the temperature

diffraction data. Figure 5b shows the refined values of the (*a*) and (*c*) cell parameters and the corresponding pseudocubic cell parameter ($\sqrt[3]{a^2c}$) (the cube root of the unit cell volume) versus the temperature.

In Fig. 5b, we can see that at the beginning there is a slow growth in (*a*), while the cell parameter (*c*) is nearly constant. At the transition temperature of 170 °C an abrupt decrease of (*c*) takes place, after which the *c/a* ratio drops to its cubic-phase value close to unity. At room temperature, the *c/a* ratio was calculated to be 1.0138, i.e., the bulk tetragonal phase.

On the other hand, the virtual cell volume and/or the cube root of the unit-cell volume increases during heating to 150 °C and then decreases by about 0.01% at the Curie point. This cell-volume decrease matches with the anomaly in the shrinkage of C2 at the Curie point as shown in Fig. 6.

To consider the ferroelectric phase-transition-assisted anomaly (FPTAA) in electric resistivity of ceramic composites it is necessary to follow the key behavior of the constituents of the composite: (i) that at least one constitutive highly resistive phase exhibits a ferroelectric transition associated with a sudden change of the lattice parameters to $a/c \approx 1$ at T_C, Fig. 5b and (ii) that at the same temperature the composite shows a discontinuity in its thermal expansion, Fig. 6.

This behavior is notable and must also take place in composites C1, C3 during heating. The grains of B′ (bright phase) embedded in the matrix of the conducting phase (dark phase) in Fig. 2a must undergo at T_C a fast drop of *c/a* ratio to unity. This ferroelectric transition causes the geometry changes of the B′ crystallites/grains in the two-phase system and simultaneously a discontinuity in the thermal expansion at T_C, Fig. 6. The volume decrease of the composite takes solely at the expense of the B′ phase transition at T_C where also the PTCR effect associated with the composite shrinkage occurs. Namely,
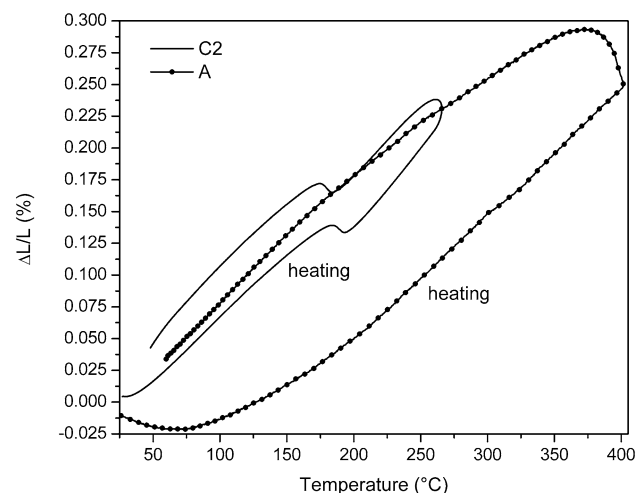
the semiconducting BT does not exhibit any geometrical change in this temperature range rather than a gradually dilatation going in parallel with B′ phase up to T_C and cannot contribute to the thermal expansion discontinuity, Fig. 6.

In other words, the rapid volume decrease of the composite can be connected with the lattice volume shrinkage during the sudden geometry change of the B′ crystallites, $c/a \Rightarrow 1$. In addition, during the grain shape change, a relatively large absolute shrinkage of the crystals/grains in the c-axis direction can break up a large part of the conductive paths of the semiconducting BT grains.

So, the proposed mechanism above may lead to a disconnection of the conducting network, i.e., the dark phase A, Fig. 2a, leading to an abrupt increase in the resistivity causing the PTCR effect and is justified to be called ferroelectric phase-transition-assisted anomaly in electric resistivity (FPTAA).

4 Conclusions

The PTCR effect in $BaTiO_3$–$(Bi_{1/2}Na_{1/2})TiO_3$ ceramics is based on a mechanism that is connected with the grain remodeling during the ferroelectric phase transition and was named ferroelectric phase transition assisted anomaly in electric resistivity (FPTAA). The name was coined on the basis of the key occurrences for the PTCR anomaly, i.e., a ferroelectric phase transition and electric resistivity anomaly. So, the resistivity peaks exclusively when the Curie temperature is reached and is not connected with any grain-boundary effect. As in the former cases of our work [9], and here, two kinds of constitutive phases must be present, i.e., a conducting phase forming a conductive network and a ferroelectric high-resistivity phase that disconnects the conducting grains/network due to its thermal expansion discontinuity at the ferroelectric phase transformation.

Fig. 6 Thermal expansion curves of the composite C2 and conducting BT as (*A*) (sintered in nitrogen, during heating and cooling)

References

1. H. Takeda, W. Aoto, T. Shiosaki, Appl. Phys. Lett. **87**, 102104 (2005)
2. T. Shimada, K. Touji, Y. Katsuyama, H. Takeda, T. Shiosaki, J. Eur. Ceram. Soc. **27**, 3877 (2007)
3. P.-H. Xiang, H. Takeda, T. Shiosaki, Jpn. J. Appl. Phys. **46**, 6995 (2007)

4. P.-H. Xiang, H. Takeda, T. Shiosaki, Appl. Phys. Lett. **91**, 162904 (2007)
5. X. Liu, X. Tan, J. Am. Ceram. Soc. **96**, 3425 (2013)
6. Y. Kaneko, F. Azough, T. Kida, K. Ito, T. Shimada, T. Minemura, B. Schaffer, R. Freer, J. Am. Ceram. Soc. **95**, 3928 (2012)
7. R.W. Cheary, A. Coelho, J. Appl. Crystallogr. **25**, 109 (1992)
8. G.A. Smolensky, V.A. Isupov, A.I. Agranovskaya, N.N. Krainik, Trans. Sov. Phys. Solid State **2**, 2651 (1961)
9. I. Zajc, M. Drofenik, Ceram. Int. **40**, 8033 (2014)